Synthesis, Characterization, and Biological Evaluation of Oxadiazole Derivatives Bearing 5-Phenyl-tetrazole as Osteoclast Differentiation Inhibitors

Seong-Hee Moon,[†,‖] Muhammad Latif,[‡,‖] Muhammad Qasim,[§] Sik-Won Choi,[†] Joo Yun Lee,[¶] Byung Jin Byun,[¶] Aamer Saeed,[§,*] and Seong Hwan Kim[†,*]

[†]*Laboratory of Translational Therapeutics, Korea Research Institute of Chemical Technology, Daejeon 305-600, Republic of Korea. *E-mail: hwan@krict.re.kr*
[‡]*Center for Catalytic Hydrocarbon Functionalization, Institute for Basic Science (IBS) and Department of Chemistry, Korea Advanced Institute of Science and Technology (KAIST), Daejeon 305-701, Korea*
[§]*Department of Chemistry, Quaid-I-Azam University, Islamabad 45320, Pakistan. *E-mail: aamersaeed@yahoo.com*
[¶]*Drug Discovery Platform Technology Group, Korea Research Institute of Chemical Technology, Daejeon 305-600, Republic of Korea*
Received April 24, 2015, Accepted May 15, 2015, Published online August 12, 2015

Novel oxadiazoles bearing 5-phenyl-tetrazole (**5a–k**) were designed and efficiently synthesized by treating 2-(5-phenyl-2*H*-tetrazole-2-yl)acetohydrazide (**4**) with aromatic carboxylic acids in $POCl_3$, and their *in vitro* anti-osteoclastogenic activities were evaluated. In the cell-based osteoclast differentiation model, all compounds (**5a–k**) inhibited the formation of osteoclasts. In addition, the potential target molecules of compound **5** analogs were predicted with their chemical substructures via a web-based interface, and some of them were found to be related to osteoclast differentiation. Consequently, the scaffold containing oxadiazole–tetrazole in a single molecule and their analogs are of potential use in the design of novel anti-osteoclastogenic therapeutics.

Keywords: Bone, Osteoclastogenesis, Oxadiazole, Tetrazole

Introduction

Continuous bone remodeling by osteoclast-mediated resorption and osteoblast-mediated mineralization (or bone formation) maintains the bone's density and strength. However, an imbalance of bone remodeling due to the overactivation of osteoclasts and/or their weakness results in bone loss, which consequently leads to pathological bone-related disorders, such as osteoporosis, rheumatoid arthritis, periodontal disease, and cancer bone metastasis.[1–4] Especially, bone-related disorders accompanied by subsequent fractures impact clinical and public health because fractures are one of the most common causes of disability and are associated with enormous healthcare expenditure.[5]

Since mature tartrate-resistant acid phosphatase (TRAP)-positive multinucleated osteoclast cells ($TRAP^+$-MNCs) derived from bone-marrow-derived macrophages (BMMs) by receptor activator of nuclear factor-κB ligand (RANKL) mediate bone resorption and their lifespan is shorter than that of osteoblasts, the therapeutic strategy to inhibit osteoclast differentiation and/or resorption is important to prevent and treat bone-related disorders.[6]

The synthesis of the heterocyclic core is of immense value in medicinal chemistry, and the intense drive for novel biologically active molecules has resulted in the never-ending search to generate libraries for biological screening.[7] The oxadiazole ring skeleton is an attractive structural motif due to its biological and pharmacological activity and is generally considered among the privileged heterocyclics due to its large impact in drug discovery programs against numerous diseases.[8–12] Typically, the privileged scaffolds of 1,3,4-oxadiazoles are very good bioisosteres (surrogates) of amides and esters, which contribute substantially to increased pharmacological activity. Because of the promising potential of 1,3,4-oxadiazoles to engage in H-bonding interactions with the receptors and promising metabolic profiles, numerous biological activities such as antitumor,[13] antimicrobial, antimitotic,[14] antifungal,[15] antihypertensive,[16] anticonvulsant,[17] antiinflammatory,[18–20] and muscle relaxant[21] have been reported.[22] Interestingly, among the four isomers of oxadiazoles, 1,3,4- oxadiazole core is a key building block in several therapeutic agents, such as furamisole (as nitrofuran antibacterial agent), nesapidil (antiarrhythmic agent), tiodazosin (antihypertensive agent), raltegravir (antiretroviral agent used for the treatment of HIV infection), translarna (used for treating patients with nonsense mutation Duchenne muscular dystrophy), and zibotentan (anticancer agent).[23]

Tetrazole with highest nitrogen content is another privileged stable scaffold. Despite the fact that tetrazole does not occur naturally, several novel drugs such as TAK-456

‖ These authors contributed equally to this work.

Correction added on 01 October 2015, after first online publication: ISSN (Print) has been corrected.

(antifungal agent),[24,25] losartan, irbesartan (angiotensin II receptor antagonists),[26] anti-inflammatory compounds,[27] antimycobacterial compounds,[28] and antihypertensive agents[29] contain tetrazole ring as a structural fragment. However, the use of 2,5-disubstituted tetrazoles as biological agents has not been reported well, but, because of its resistance to biological degradation, it is possible to use this structural motif as isosteric substituents of various functional groups in the development of biologically active substances. To this end, 2,5-disubstituted tetrazoles as glutamate receptor modulators[30] and antiviral viral agents have been reported a decade ago.[31,32]

Keeping in view the individual significance of both oxadiazole and tetrazole pharmacophores, here we report the synthesis of tetrazole–oxadiazole conjugates (**5a–k**) incorporating the tetrazole and oxadiazole units connected through one carbon bridge as anti-osteoclastogenic agents. The newly synthesized oxadiazoles decorated with 5-phenyltetrazoles hybrids were investigated for unmapped region of these privileged pharmacophores as osteoclast differentiation inhibitors.

Results and Discussion

Chemistry. Our study commenced with the preparation of the intermediate 5-phenyl-*2H*-tetrazole (**2**) from readily available benzonitrile (**1**), as shown in Scheme 1. The substrate, 5-phenyl-*2H*-tetrazole (**2**), was further alkylated with methyl chloroacetate to provide methyl 2-(5-phenyl-*2H*-tetrazol-2-yl)acetate (**3**) in 73% yield, followed by its conversion into the corresponding 2-(5-phenyl-*2H*-tetrazol-2-yl)acetohydrazide (**4**) in excellent yield. The heterocyclization to asymmetrical 2,5-diaryl(alkyl)-1,3,4-oxadiazoles (**5a–k**) was accomplished through the condensation of acyl hydrazide (**4**) with suitably substituted aromatic carboxylic acids in presence of phosphorous oxychloride.

Biology. Inhibitory effect of **5a–k** on the formation of osteoclasts. The effect of **5a–k** on osteoclast differentiation was evaluated by counting TRAP$^+$-MNCs after BMMs were treated with each compound in the presence of RANKL and cultured for 4 days. TRAP is a well-known biomarker of osteoclast differentiation,[33] and the fusion of monocyte BMMs to form giant MNCs is required for mature osteoclasts to functionally resorb bone.[34] As shown in Table 1, RANKL induced the differentiation of BMMs into 181 TRAP$^+$-MNCs, but **5a–k** at 10 μM significantly inhibited the formation of TRAP$^+$-MNCs. Compound **5k** exhibited the strongest anti-osteoclastogenic activity.

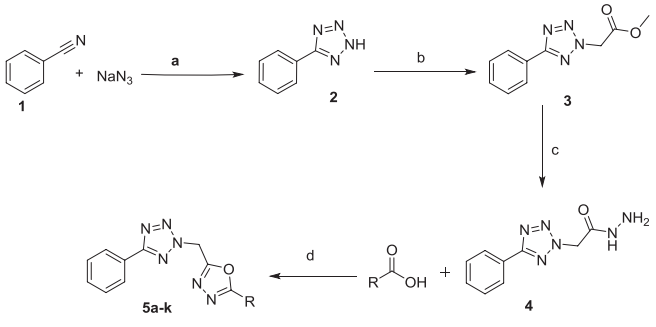

Reagents and conditions: (a) $ZnCl_2$, H_2O, HCl, 15 h, 78% (b) Methyl chloroacetate, Et_3N, CH_3CN, reflux, 2 h, 73% (c) MeOH, $NH_2NH_2.H_2O$, 95% (d) $POCl_3$, reflux 7-8 h

Scheme 1. Synthesis of **5a-k**.

The dose-dependent anti-osteoclastogenic activity of **5k** was further evaluated. When BMMs differentiated into TRAP$^+$-MNCs by RANKL, **5k** was shown to inhibit the formation of TRAP$^+$-MNCs in a dose-dependent manner (Figure 1(a)). No cytotoxicity in BMMs by **5k** was observed at the concentrations used in this study, suggesting that its anti-osteoclastogenic activity could not be due to the cytotoxicity (Figure 1(b)). Anti-osteoclastogenic activity of **5k** was also

Table 1. Inhibitory effect of **5a–k** on the formation of osteoclasts

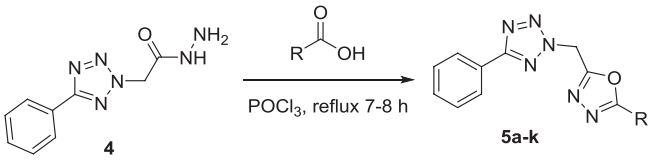

Cpds	R	No. of TRAP$^+$-MNCs (at 10 μM) (vehicle control; 181.67 ± 7.64)
5a	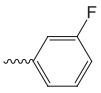	135.00 ± 2.65
5b	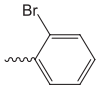	102.33 ± 24.42
5c	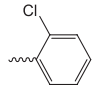	100.33 ± 1.15
5d	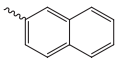	85.67 ± 6.03
5e	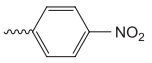	84.67 ± 22.03
5f		75.00 ± 8.72
5g		70.33 ± 12.66
5h		65.33 ± 4.51
5i	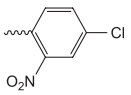	64.00 ± 7.00
5j	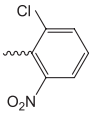	52.33 ± 7.51
5k	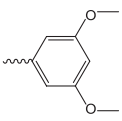	28.00 ± 16.09

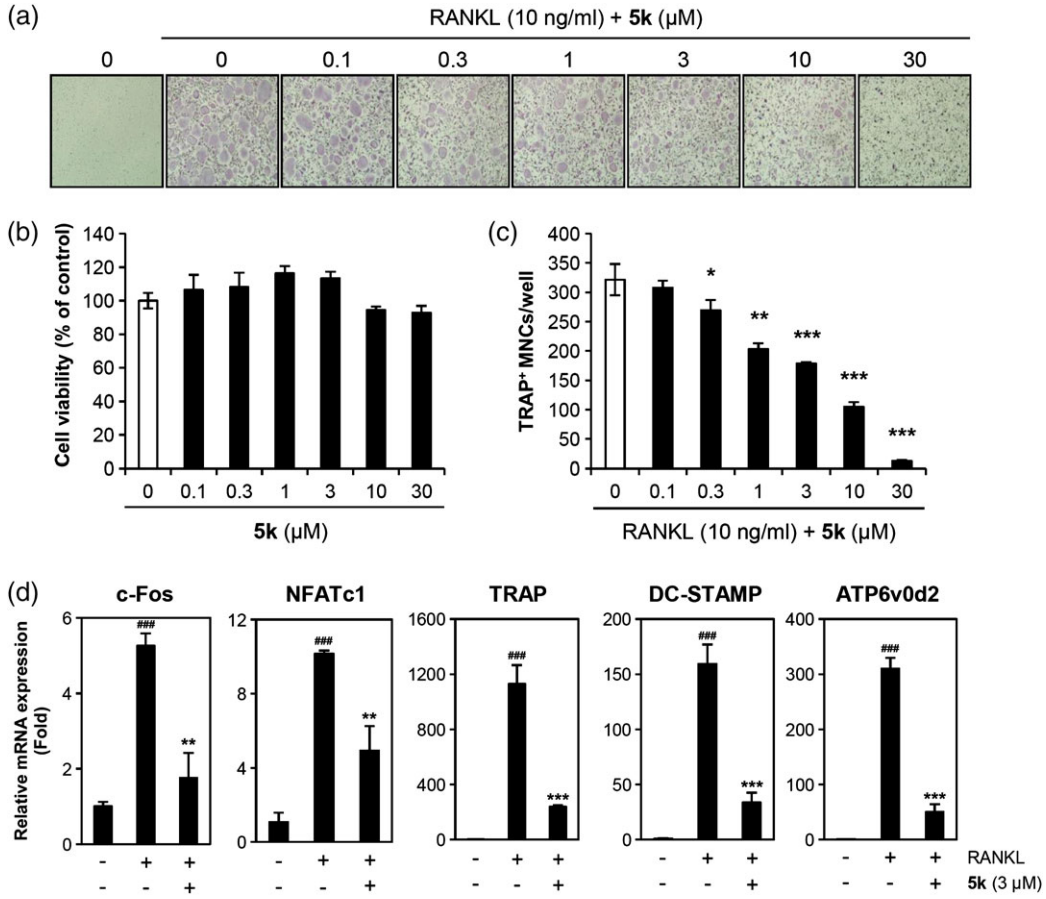

Figure 1. Anti-osteoclastogenic activity of **5k**. (A) After BMMs were cultured for 4 days in the presence of RANKL (10 ng/mL) and M-CSF (30 ng/mL) with the vehicle (0.1% DMSO) or **5k**, multinucleated osteoclasts were visualized by TRAP staining. Also, the effect of **5k** on the viability of BMMs (B), the formation of $TRAP^+$-MNCs (C), and mRNA expression levels of gene related to osteoclast differentiation (D) were evaluated as described in "Materials and Methods".$^{###}$, $P < 0.001$ (vs. the negative control); *, $P < 0.05$; **, $P < 0.01$; ***, $P < 0.001$ (vs. the RANKL-treated group).

confirmed by counting the number of $TRAP^+$-MNCs (Figure 1(c)) and measuring the mRNA expression levels of the gene related to osteoclast differentiation such as c-Fos, nuclear factor of activated T cells c1 (NFATc1), TRAP, the dendritic cell-specific transmembrane protein (DC-STAMP), and the d2 isoform of vacuolar (H+) ATPase V0 domain (ATP6v0d2).

Two main transcription factors, c-Fos and NFATc1, are induced by RANKL in the early-to-middle and middle-to-late stages of osteoclast differentiation, respectively.[35] The temporal induction of these transcription factors plays a role in the transcriptional regulation of specific genes related to osteoclast differentiation, migration, fusion, and/or resorption. Especially, DC-STAMP and ATP6v0d2 contain multiple NFATc1 binding sites in their promoter regions,[36] and the proteins encoded by both of these genes are reported to play roles in osteoclast fusion.[37,38]

***In silico* Target Prediction.** In order to predict the biological targets of compound **5** analogs, the chemicals with the similar substructure as compound **5** analogs were identified in the ChEMBL database.[39] As shown in Table 2, two proteins, carboxypeptidase B and P2X purinoceptor 7 (P2X7), were identified as the potential binding partners of compound **5** analogs, and five proteins, namely histone-lysine *N*-methyltransferase, H3 lysine-9 specific 3 (G9a), glucagon-like peptide 1 receptor (GLP-1R), prelamin-A/C, DNA polymerase β, and voltage-gated T-type calcium channel α-1H subunit, were identified as potential functional molecules to show the biological activity of compound **5** analogs. Among them, the inhibition of P2X7 or G9a has been shown to block osteoclast differentiation. P2X7 expression in osteoclasts has been reported,[40] and RAW264.7 cells that lacked P2X7 function have been shown to fail to fuse to form multinucleated osteoclasts in response to RANKL.[41] The structural similarity between **5k** and the P2X7 antagonist CHEMBL1096099 was calculated to be about 61%. BIX01294, a specific inhibitor of G9a, suppressed osteoclast differentiation.[42] In a further study, the involvement of P2X7 or G9a in the anti-osteoclastogenic action of compound **5** analogs would be investigated in detail.

Experimental

Chemistry. All chemicals were reagent grade and used as purchased. Reactions were monitored by TLC. Flash column

Table 2. Target prediction for **5k**.

CHEMBLID	Structure	Target protein (UnitProtKB)
1. Assay plate form: Binding assay		
CHEMBL552336	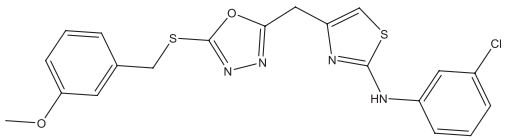	Carboxypeptidase B (P15086)
CHEMBL1096099	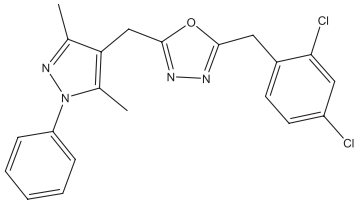	P2X purinoceptor 7 (Q99572)
2. Assay plate form: Functional assay		
CHEMBL1318385	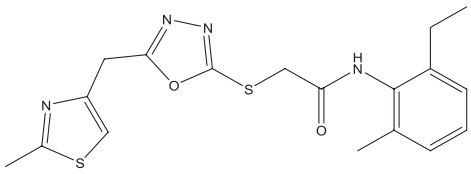	Histone-lysine *N*-methyltransferase, H3 lysine-9 specific 3 (Q96KQ7)
CHEMBL1310954	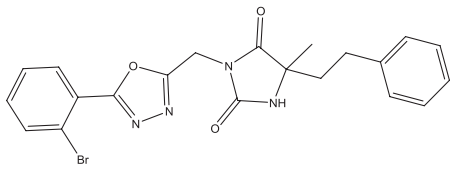	Glucagon-like peptide 1 receptor (P43220) Prelamin-A/C (P02545) DNA polymerase beta (P06746)
CHEMBL1408371	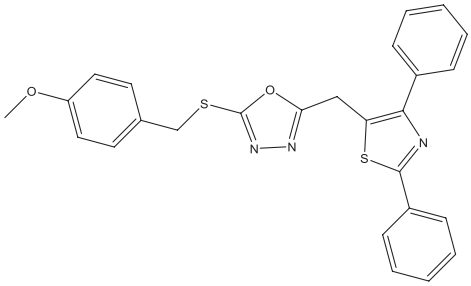	Glucagon-like peptide 1 receptor (P43220) Voltage-gated T-type calcium channel alpha-1H subunit (O95180)

chromatography was carried out on silica gel (230–400 mesh). ^{1}H NMR and ^{13}C NMR spectra were recorded in δ units relative to deuterated solvent as an internal reference using a 500 MHz NMR instrument. Liquid chromatography-tandem mass spectrometry analysis was performed on an electrospray ionization (ESI) mass spectrometer with photodiode-array detector (PDA) detection (Scheme 2).

Synthesis of 5-Phenyl-*2H*-tetrazole (2). A mixture of sodium azide (17.05 g, 262 mmol), benzonitrile (25.75 g, 250 mmol), and zinc (II) chloride (17 g, 120 mmol) was suspended in H_2O (250 mL). The reaction mixture was refluxed for 15 h. After consumption of benzonitrile, the mixture was cooled to room temperature and filtered. The solid residue was treated with 3 N HCl (250 mL) to give the desired product **2** as a white crystalline solid (21.0 g, 78% yield). Mp 216 °C: ^{1}H NMR (300 MHz, DMSO-d_6) δ 7.59–7.62 (m, 3H), 8.02–8.06 (m, 2H). LC-MS (EI) for $C_7H_6N_4$ $(M+H)^+$: m/z = 147.06, Exact mass:146.06 (Scheme 3).

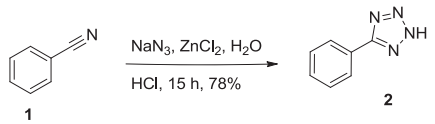

Scheme 2. Synthesis of probe **2**.

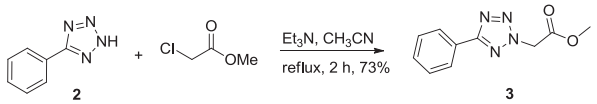

Scheme 3. Synthesis of probe **3**.

Preparation of Methyl 2-(5-phenyl-*2H*-tetrazole-2-yl)acetate (3). A mixture of 5-phenyl-tetrazole 2 (18.26 g, 120 mmol), triethyl amine (50.59 g, 500 mmol), and methyl chloroacetate (27.13 g, 250 mmol) was refluxed in 150 mL of

acetonitrile was refluxed for 2 h. The completion of reaction was checked by TLC. On completion of the reaction, the solvent was removed under reduced pressure and the solid product obtained was recrystallized from *n*-hexane to furnish the pure methyl 2-(5-phenyl-*2H*-tetrazole-1-yl)acetate **3** (25 g, white crystalline solid) in 73% yield. Mp 98–100 °C; FT-IR (neat) ν (cm^{-1}): 1281 (N=N–N), 1547 (Ar–C=C), 1606 (C=N), 1756 (C=O), 2854 (CH_3), 3067 (Ar–CH); 1H NMR (300 MHz, DMSO-d_6) δ 3.75 (s, 2H), 5.93 (s, 2H), 7.56-7.59 (m, 3H), δ 8.06-8.10 (m, 2H). LC-MS (EI) for $C_{10}H_{10}N_4O_2$ $(M+H)^+$: m/z = 219.09, Exact mass:218.0804.

Preparation of 2-(5-Phenyl-*2H*-tetrazole-2-yl)acetohydrazide (4). To a solution of methyl 2-(5-phenyl-*2H*-tetrazole-2-yl)acetate **3** (27.25 g, 125 mmol) in 150 mL of anhydrous methanol was added hydrazine hydrate (12.50 g, 250 mmol). The reaction mixture was stirred at room temperature and the progress monitored by TLC. On completion, the product precipitated out, which was filtered and washed with methanol to leave product **4** as white crystalline powder. Mp 212 °C: FT-IR (neat) ν (cm^{-1}): 1280 (N=N–N), 1549 (Ar–C=C), 1608 (C=N), 1659 (C=O), 3057 (Ar–CH), 3132 (N–H), 3307 (NH2); ^{1}H NMR (300 MHz, DMSO-d_6) δ 4.46 (s, 2H), 5.45 (s, 2H), 7.55–7.61 (m, 3H), 8.05–8.08 (m, 2H), 9.65 (s, 1H). LC-MS (EI) for $C_9H_{10}N_6O$ $(M+H)^+$: m/z = 219.09, Exact mass: 218.0916 (Scheme 4).

General Procedure for the Synthesis of 2-Phenyl-5-((5-phenyl-*2H*-tetrazol-2-yl)methyl)-1,3,4-oxadiazoles (5a–k). An equimolar mixture of 2-(5-phenyl-*2H*-tetrazole-2-yl) acetohydrazide **4** and the suitable carboxylic acid in phosphorous oxychloride was refluxed for 7–8 h. The progress of reaction was continuously monitored by TLC. On completion, the reaction mixture was poured onto ice slowly. The reaction mixture was neutralized with a 5% solution of potassium carbonate and was allowed to stand in a freezer for 1 h. The product that precipitated out was filtered and washed with cold water several times to afford the desired series of compounds (**5a–k**) (Scheme 5).

2-(3-Fluorophenyl)-5-((5-phenyl-*2H*-tetrazol-2-yl) methyl)-1,3,4-oxadiazole (5a): White crystalline solid (Yield: 91%), Mp. 233–236 °C; FT-IR (neat) ν (cm^{-1}): 1058 (C–O–C), 1280 (N=N–N), 1549 (Ar–C=C), 1608 (C=N), 3057 Ar-CH); ^{1}H NMR (300 MHz, DMSO-d_6) δ 5.55 (s, 2H), 7.44–7.75 (m, 7H), 8.09 (m, 2H); LC-MS (EI) for $C_{16}H_{11}FN_6O$ $(M+H)^+$: m/z = 323.30, Exact mass: 322.0978.

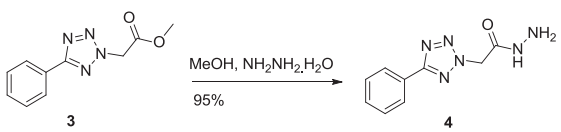

Scheme 4. Synthesis of probe **4**.

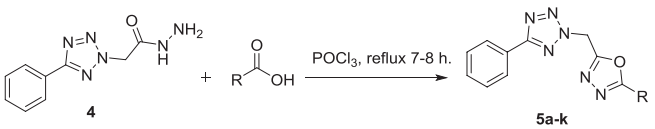

Scheme 5. Synthesis of **5a–k**.

2-(2-Bromophenyl)-5-((5-phenyl-*2H*-tetrazol-2-yl) methyl)-1,3,4-oxadiazole (5b): Light brown solid (Yield: 90%), mp. 257–260 °C; FT-IR (neat) ν (cm^{-1}): 1159 (C–O–C), 1285 (N=N–N), 1540 (Ar–C=C), 695 (–C–Br), 1611 (C=N), 3057 (Ar–CH); ^{1}H NMR (300 MHz, DMSO-d_6) δ 5.63 (s, 2H), 7.32–8.01 (m, 7H), 8.03 (m, 2H); LC-MS (EI) for $C_{16}H_{11}BrN_6O$ $(M+H)^+$: m/z = 383.12, Exact mass: 382.0177.

2-(2-Chlorophenyl)-5-((5-phenyl-*2H*-tetrazol-2-yl)methyl)-1,3,4-oxadiazole (5c): Yellowish solid (Yield: 82%), Mp. 232–235 °C; FT-IR (neat) ν (cm^{-1}): 1060 (C–O–C), 1280 (N=N–N), 1553 (Ar–C=C), 780 (–C–Cl), 1610 (C=N), 3060 (Ar–CH); ^{1}H NMR (300 MHz, DMSO-d_6) δ 5.71 (s, 2H), 7.42–7.31 (m, 6H), 8.10 (m, 3H); LC-MS (EI) for $C_{16}H_{11}C_lN_6O$ $(M+H)^+$: m/z = 339.07, Exact mass: 338.0682.

2-(2-Naphthyl)-5-((5-phenyl-*2H*-tetrazol-2-yl)methyl)-1,3,4-oxadiazole (5d): White crystalline solid (Yield: 95%), Mp. 242–245 °C; FT-IR (neat) ν (cm^{-1}): 1055 (C–O–C), 1280 (N=N–N), 1549 (Ar–C=C), 1608 (C=N), 3057 (Ar–CH); ^{1}H NMR (300 MHz, DMSO-d_6) δ 5.61 (s, 2H), 7.82–8.18 (m, 9H), 8.26 (m, 2H), 8.91 (s, 1H); LC-MS (EI) for $C_{20}H_{14}N_6O$ $(M+H)^+$: m/z = 355.36, Exact mass: 354.1229.

2-(4-Nitrophenyl)-5-((5-phenyl-*2H*-tetrazol-2-yl)methyl)-1,3,4-oxadiazole (5e): Light green solid (Yield: 95%), Mp. 245–247 °C; FT-IR (neat) ν (cm^{-1}): 1020 (C–O–C), 1282 (N=N–N), 1549 (Ar–C=C), 1564 (–NO2), 1616 (C=N), 3057 (Ar–CH); ^{1}H NMR (300 MHz, DMSO-d_6) δ 5.75 (s, 2H), 7.57 (m, 3H), 8.01-8.21 (m, 4H), 8.36 (d, J = 5.5 Hz, 2H); LC-MS (EI) for $C_{16}H_{11}BrN_7O_3$ $(M+H)^+$: m/z = 350.10, Exact mass: 349.0923.

2-(tert-Butyl)-5-((5-phenyl-*2H*-tetrazol-2-yl)methyl)-1,3,4-oxadiazole (5f): Light greenish solid (Yield: 97%), Mp. 175–177 °C; FT-IR (neat) ν (cm^{-1}): 1026 (C–O–C), 1280 (N=N–N), 1608 (C=N), 3125, 3160 (N–H); ^{1}H NMR (300 MHz, DMSO-d_6) δ 1.20 (s, 9H), 5.60 (s, 2H), 7.55–7.61 (m, 3H), 8.07 (m, 2H); LC-MS (EI) for $C_{14}H_{16}N_6O$ $(M+H)^+$: m/z = 285.14, Exact mass: 284.1385.

2-(Furan-2-yl)-5-((5-phenyl-*2H*-tetrazol-2-yl)methyl)-1,3,4-oxadiazole (5g): White solid (Yield: 88%). Mp. 198–200 °C; FT-IR (neat) ν (cm^{-1}): 1142 (C–O–C), 1285 (N=N–N), 1551 (Ar–C=C), 1605 (C=N), 3072 (Ar–CH); ^{1}H NMR (300 MHz, DMSO-d_6) δ 5.64 (s, 2H), 6.64 (d, J = 3Hz, 1H), 7.2 (d, J = 3Hz, 1H), 7.62–7.90 (m, 4H), 8.04 (m, 2H); LC-MS (EI) for $C_{14}H_{10}N_6O_2$ $(M+H)^+$: m/z = 295.11, Exact mass: 294.0865.

2-((5-Phenyl-*2H*-tetrazol-2-yl)methyl)-5-(m-tolyl)-1,3,4-oxadiazole (5h): White crystalline solid (Yield: 95%), Mp. 243–245 °C; FT-IR (neat) ν (cm^{-1}): 1056 (C–O–C), 1280 (N=N–N), 1549 (Ar–C=C), 1609 (C=N), 3057 (Ar–CH); ^{1}H NMR (300 MHz, DMSO-d_6) δ 3.06 (s, 3H), 5.62 (s, 2H), 7.20–7.36 (m, 7H), 8.01 (m, 2H); LC-MS (EI) for $C_{17}H_{14}N_6O$ $(M+H)^+$: m/z = 319.11, Exact mass: 318.1229.

2-(4-Chloro-2-nitrophenyl)-5-((5-phenyl-*2H*-tetrazol-2-yl)methyl)-1,3,4-oxadiazole (5i): Light yellowish solid (Yield: 80%). Mp. 265–267 °C; FT-IR (neat) ν (cm^{-1}): 1035 (C–O–C), 1280 (N═N–N), 1549 (Ar–C═C), 782 (–C–Cl), 1560 (–NO2), 1610 (C═N), 3057 (Ar–CH); ^{1}H NMR (300 MHz, DMSO-d_6) δ 5.60 (s, 2H), 7.53-8.17 (m, 5H), 8.24 (m, 2H), 8.43 (s, 1H); LC-MS (EI) for $C_{16}H_{10}C_lN_7O_3$ (M +H)$^+$: m/z = 384.75, Exact mass: 383.0533.

2-(2-Chloro-6-nitrophenyl)-5-((5-phenyl-*2H*-tetrazol-2-yl)methyl)-1,3,4-oxadiazole (5j): Light yellowish solid (Yield: 80%). Mp. 275–278 °C; FT-IR (neat) ν (cm^{-1}): 1130 (C–O–C), 1280 (N═N–N), 1549 (Ar–C═C), 782 (–C–Cl), 1560 (–NO_2), 1608 (C═N), 3057 (Ar–CH); ^{1}H NMR (300 MHz, DMSO-d_6) δ 5.74 (s, 2H), 7.35 (m, 1H), 7.57 (m, 3H), 8.05 (m, 2H), 8.25 (d, J = 3Hz, 1H), 8.36 (d, J = 3Hz, 1H); LC-MS (EI) for $C_{16}H_{10}C_lN_7O_3$ (M+H)$^+$: m/z = 384.15, Exact Mass: 383.0533.

2-(3,5-Dimethoxyphenyl)-5-((5-phenyl-*2H*-tetrazol-2-yl)methyl)-1,3,4-oxadiazole (5k): White solid (Yield: 76%). Mp. 263–266 °C; FT-IR (neat) ν (cm^{-1}): 1026 (C–O–C), 1280 (N═N–N), 1552 (Ar–C═C), 1220 (ArC–O–C), 1608 (C═N), 3055 (Ar–CH); ^{1}H NMR (300 MHz, DMSO-d_6) δ 3.82 (s, 6H), 5.70 (s, 2H), 6.69 (s, 1H), 7.03 (s, 2H), 7.57 (m, 3H), 8.07 (m, 2 H); LC-MS (EI) for $C_{18}H_{16}N_6O_3$ (M+H)$^+$: m/z = 365.15, Exact mass: 364.1283.

Biology

Osteoclast Differentiation. This study was carried out in strict accordance with the recommendations in the Standard Protocol for Animal Study of Korea Research Institute of Chemical Technology (KRICT; No. 2012-7D-02-01). The protocol (ID No. 7D-M1) was approved by the Institutional Animal Care and Use Committee of KRICT. All efforts were made to minimize suffering for the animals. Five-week-old male ICR mice (Damul Science Co., Daejeon, Korea) were maintained in a room illuminated daily from 07:00 to 19:00 (a 12:12 h light/dark cycle) under controlled temperature (23 ± 1 °C) and ventilation (10–12 times per hour). Humidity was maintained at 55 ± 5%, and the mice had free access to a standard animal diet and tap water. To isolate bone-marrow-derived cells (BMCs) from mice, after cervical dislocation, femur and tibia were flushed with α-MEM (Invitrogen Life Technologies, Carlsbad, CA, USA) supplemented with antibiotics (100 Units/mL penicillin and 100 μg/mL streptomycin; Invitrogen Life Technologies, Grand Island, NY, USA). BMCs were cultured on a culture dish in α-MEM supplemented with 10% fetal bovine serum (FBS; Invitrogen Life Technologies, Grand Island, NY, USA) with 10 ng/mL of mouse recombinant M-CSF (R&D Systems, Minneapolis, MN, USA) for 1 day. Then, after nonadherent BMCs were re-plated on a Petri dish and cultured for 3 days in the presence of M-CSF (30 ng/mL), the adherent BMMs were used for osteoclast differentiation. For osteoclastogenesis, BMMs (1×10^4 cells/well in a 96-well plate or 3×10^5 cells/well in a 6-well plate) were seeded in triplicate and cultured in the presence of 10 ng/mL of mouse recombinant RANKL (R&D Systems) and M-CSF (30 ng/mL) for 4 days to differentiate into mature TRAP$^+$-MNCs.

TRAP Staining and Osteoclast Counting. Mature osteoclasts were visualized by staining TRAP, a biomarker of osteoclast differentiation. Briefly, multinucleated osteoclasts were fixed with 3.7% formalin for 10 min, permeabilized with 0.1% Triton X-100 for 10 min, and stained with TRAP solution (Sigma-Aldrich, MO, USA). TRAP$^+$-MNCs (≥5 nuclei) were then counted.

Cell Viability Assay. BMMs (1×10^4 cells/well) were seeded in a 96-well plate and incubated for 1 day. Then, cells were treated with M-CSF (30 ng/mL) and **5k**. After incubation for 3 days, cell viability was measured by the CCK-8 assay kit according to the manufacturer's protocol. All experiments were performed in triplicate.

Evaluation of mRNA Expression. In the presence of M-CSF (30 ng/mL), BMMs were treated with RANKL (10 ng/mL) or its combination with **5k** (3 μM) for 3 days. Then, total RNA was isolated using TRIzol reagent (Life Technologies, Grand Island, NY, USA) and the first-strand cDNA was synthesized using 1 μg of total RNA, 1 μM of oligo-dT_{18} primer, 10 units of the RNase inhibitor, RNasin (Promega, Madison, WI, USA), and Omniscript Reverse Transcriptase (Qiagen, Valencia, CA, USA) according to the manufacturer's instruction. SYBR green-based quantitative PCR was performed using the Stratagene Mx3000P real-time PCR system in 20 μL reaction mixture containing 10 μL of TOPreal qPCR 2× PreMIX (Enzynomics, Daejeon, Korea), 2 pmol of forward primer, 2 pmol of reverse primer, and 2 μL of 1:10-diluted first-strand cDNA 1 μg of cDNA. Amplification parameters consisted of an initial denaturation at 95 °C for 10 min and 40 cycles of three-step PCR (a denaturation at 94 °C for 40 s, annealing at 53 °C for 40 s, and extension at 72 °C for 1 min). All reactions were run in triplicate, and the data were analyzed using the $2^{-\Delta\Delta CT}$ method.[43] Primers were designed using an online primer design program (Table 3).[44] GAPDH was used as the control gene. Significance was determined with GAPDH-normalized $2^{-\Delta\Delta CT}$ values.

Table 3. Primer sequences used in this study.

Target Gene	Forward Primer (5′–3′)	Reverse Primer (5′–3′)
c-Fos	CCAGTCAAGAGCATCAGCAA	AAGTAGTGCAGCCCGGAGTA
NFATc1	GGGTCAGTGTGACCGAAGAT	GGAAGTCAGAAGTGGGTGGA
TRAP	GATGACTTTGCCAGTCAGCA	ACATAGCCCACACCGTTCTC
DC-STAMP	CCAAGGAGTCGTCCATGATT	GGCTGCTTTGATCGTTTCTC
ATP6v0d2	AGACCACGGACTATGGCAAC	CGATGGGTGACACTTGGCTA
GAPDH	AACTTTGGCATTGTGGAAGG	ACACATTGGGGGTAGGAACA

Computational Methods. Based on the chemical substructure, target molecules for compound **5** analogs were predicted via a web-based interface at https://www.ebi.ac.uk/chembl.[39] Active compounds containing the 1,3,4-oxadiazole moieties connected to the five-membered heterocyclic rings through a carbon linker were chosen for the target prediction. The structural similarity was calculated by ECFC4 method in Pipeline Pilot, version 8.5 (Accelrys, San Diego, CA, USA).

Conclusions

In conclusion, we synthesized novel oxadiazoles bearing 5-phenyl-tetrazole analogs, found their anti-osteoclastogenic activities, and suggested P2X7 or G9a as their target molecules *in silico*. In future, we propose to study the structural tuning of oxadiazoles bearing 5-phenyl-tetrazole to fit one of the potential target molecules related to osteoclast differentiation, which might improve their target specificity and anti-osteoclastogenic activity.

References

1. H. Takayanagi, *Nat. Rev. Rheumatol.* **2009**, *5*, 667.
2. J. A. Cirelli, C. H. Park, K. MacKool, M. Taba Jr., K. H. Lustig, H. Burstein, W. V. Giannobile, *Gene Ther.* **2009**, *16*, 426.
3. A. Daroszewska, S. H. Ralston, *Nat. Clin. Pract. Rheumatol.* **2006**, *2*, 270.
4. B. K. Park, H. Zhang, Q. Zeng, J. Dai, E. T. Keller, T. Giordano, K. Gu, V. Shah, L. Pei, R. J. Zarbo, L. McCauley, S. Shi, S. Chen, C. Y. Wang, *Nat. Med.* **2007**, *13*, 62.
5. NIH Consensus Development Panel on Osteoporosis Prevention, Diagnosis, and Therapy, *JAMA* **2001**, *285*, 785.
6. W. J. Boyle, W. S. Simonet, D. L. Lacey, *Nature* **2003**, *423*, 337.
7. J. Bostrom, A. Hogner, A. Llinas, E. Wellner, A. T. Plowright, *J. Med. Chem.* **2012**, *55*, 1817.
8. D. M. Cottrell, J. Capers, M. M. Salem, K. DeLuca-Fradley, S. L. Croft, K. A. Werbovetz, *Bioorg. Med. Chem. Lett.* **2004**, *12*, 2815.
9. R. M. Jones, J. N. Leonard, D. J. Buzard, J. Lehmann, *Expert Opin. Ther. Pat.* **2009**, *19*, 1339.
10. S. H. Lee, H. J. Seo, S. H. Lee, M. E. Jung, J. H. Park, H. J. Park, J. Yoo, H. Yun, J. Na, S. Y. Kang, K. S. Song, M. A. Kim, C. H. Chang, J. Kim, J. Lee, *J. Med. Chem.* **2008**, *51*, 7216.
11. R. Raza, A. Saeed, M. Arif, S. Mahmood, M. Muddassar, A. Raza, J. Iqbal, *Chem. Biol. Drug Des.* **2012**, *80*, 605.
12. H. Z. Zhang, S. Kasibhatla, J. Kuemmerle, W. Kemnitzer, K. Ollis-Mason, L. Qiu, C. Crogan-Grundy, B. Tseng, J. Drewe, S. X. Cai, *J. Med. Chem.* **2005**, *48*, 5215.
13. S. Valente, D. Trisciuoglio, T. De Luca, A. Nebbioso, D. Labella, A. Lenoci, D. Bigogno, G. Dondio, M. Miceli, G. Brosch, D. Del Bufalo, L. Altucci, A. Mai, *J. Med. Chem.* **2014**, *57*, 6259.
14. K. M. Rai, N. Linganna, *Farmaco* **2000**, *55*, 389.
15. L. Li, H. Ding, B. Wang, S. Yu, Y. Zou, X. Chai, Q. Wu, *Bioorg. Med. Chem. Lett.* **2014**, *24*, 192.
16. S. Turner, M. Myers, B. Gadie, A. J. Nelson, R. Pape, J. F. Saville, J. C. Doxey, T. L. Berridge, *J. Med. Chem.* **1988**, *31*, 902.
17. C. B. Chapleo, P. L. Myers, A. C. Smith, M. R. Stillings, I. F. Tulloch, D. S. Walter, *J. Med. Chem.* **1988**, *31*, 7.
18. D. H. Boschelli, D. T. Connor, D. A. Bornemeier, R. D. Dyer, J. A. Kennedy, P. J. Kuipers, G. C. Okonkwo, D. J. Schrier, C. D. Wright, *J. Med. Chem.* **1993**, *36*, 1802.
19. M. D. Mullican, M. W. Wilson, D. T. Connor, C. R. Kostlan, D. J. Schrier, R. D. Dyer, *J. Med. Chem.* **1993**, *36*, 1090.
20. F. Omar, N. Mahfouz, M. Rahman, *Eur. J. Med. Chem.* **1996**, *31*, 819.
21. H. L. Yale, K. Losee, *J. Med. Chem.* **1966**, *9*, 478.
22. T. Fang, Q. Tan, Z. Ding, B. Liu, B. Xu, *Org. Lett.* **2014**, *16*, 2342.
23. H. Khalilullah, M. J. Ahsan, M. Hedaitullah, S. Khan, B. Ahmed, *Mini Rev. Med. Chem.* **2012**, *12*, 789.
24. T. Ichikawa, M. Yamada, M. Yamaguchi, T. Kitazaki, Y. Matsushita, K. Higashikawa, K. Itoh, *Chem. Pharm. Bull. (Tokyo)* **2001**, *49*, 1110.
25. J. Adamec, R. Beckert, D. Weiss, V. Klimesova, K. Waisser, U. Mollmann, J. Kaustova, V. Buchta, *Bioorg. Med. Chem. Lett.* **2007**, *15*, 2898.
26. B. Le Bourdonnec, E. Meulon, S. Yous, J. F. Goossens, R. Houssin, J. P. Henichart, *J. Med. Chem.* **2000**, *43*, 2685.
27. D. G. Batt, G. C. Houghton, J. Roderick, J. B. Santella, D. A. Wacker, P. K. Welch, Y. I. Orlovsky, E. A. Wadman, J. M. Trzaskos, P. Davies, C. P. Decicco, C. P. Carter, *Bioorg. Med. Chem. Lett.* **2005**, *15*, 787.
28. K. Waisser, J. Adamec, J. Kunes, J. Kaustova, *Chem. Pap.* **2004**, *58*, 214.
29. W. T. Ashton, C. L. Cantone, L. C. Meurer, R. L. Tolman, W. J. Greenlee, A. A. Patchett, R. J. Lynch, T. W. Schorn, J. F. Strouse, P. K. Siegl, *J. Med. Chem.* **1992**, *35*, 2103.
30. E. Vieira, J. Huwyler, S. Jolidon, F. Knoflach, V. Mutel, J. Wichmann, *Bioorg. Med. Chem. Lett.* **2005**, *15*, 4628.
31. L. V. Myznikov, A. Hrabalek, G. I. Koldobskii, *Chem. Heterocycl. Comp.* **2007**, *43*, 1.
32. C. S. Chang, Y. T. Lin, S. R. Shih, C. C. Lee, Y. C. Lee, C. L. Tai, S. N. Tseng, J. H. Chern, *J. Med. Chem.* **2005**, *48*, 3522.
33. A. R. Hayman, *Autoimmunity* **2008**, *41*, 218.
34. M. S. Lee, H. S. Kim, J. T. Yeon, S. W. Choi, C. H. Chun, H. B. Kwak, J. Oh, *J. Immunol.* **2009**, *183*, 3390.
35. S. W. Choi, Y. J. Son, J. M. Yun, S. H. Kim, *eCAM* **2012**, *2012*, 810563.
36. K. Kim, S. H. Lee, J. Ha Kim, Y. Choi, N. Kim, *Mol. Endocrinol.* **2008**, *22*, 176.
37. S. H. Lee, J. Rho, D. Jeong, J. Y. Sul, T. Kim, N. Kim, J. S. Kang, T. Miyamoto, T. Suda, S. K. Lee, R. J. Pignolo, B. Koczon-Jaremko, J. Lorenzo, Y. Choi, *Nat. Med.* **2006**, *12*, 1403.
38. T. Miyamoto, *Mod. Rheumatol.* **2006**, *16*, 341.
39. A. Gaulton, L. J. Bellis, A. P. Bento, J. Chambers, M. Davies, A. Hersey, Y. Light, S. McGlinchey, D. Michalovich, B. Al-Lazikani, J. P. Overington, *Nucleic Acids Res.* **2012**, *40*, D1100.
40. A. Hoebertz, A. Townsend-Nicholson, R. Glass, G. Burnstock, T. R. Arnett, *Bone* **2000**, *27*, 503.
41. J. F. Hiken, T. H. Steinberg, *Am. J. Physiol. Cell Physiol.* **2004**, *287*, C403.
42. H. Tsuda, N. Zhao, K. Imai, K. Ochiai, P. Yang, N. Suzuki, *Bosn. J. Basic Med. Sci.* **2013**, *13*, 271.
43. K. J. Livak, T. D. Schmittgen, *Methods* **2001**, *25*, 402.
44. S. Rozen, H. Skaletsky, *Methods Mol. Biol.* **2000**, *132*, 365.

